RESEARCH ARTICLE

An agent-based model accurately predicts larval dispersal and identifies restoration and monitoring priorities for eastern oyster (*Crassostrea virginica*) in a Southwest Florida estuary

Bass Dye[1,2,3] 🄔, Felix Jose[1] 🄔, Joëlle Richard[1,4], Jonas Brandi Mortensen[5], Eric C. Milbrandt[6] 🄔

An agent-based modeling (ABM) framework was developed to support oyster reef restoration efforts in the Caloosahatchee River Estuary located within the encompassing Charlotte Harbor estuarine system, Southwest Florida. The modeling approach is novel for this shallow estuary which experiences heavily managed freshwater inflow known to be an ecological stressor to the estuary's oysters. The aims of the study were to (1) determine the ABM's accuracy in simulating larval dispersal patterns when compared with measured in situ larval settlement data; (2) establish connectivity patterns between various oyster reefs within the estuary; and (3) discover larval transport pathways within the Charlotte Harbor estuarine system. Key characteristics of the ABM, in particular the agents serving as simulated larvae, include settlement behavior and salinity tolerance and associated mortality. The ABM accurately recreated larval dispersal patterns during the peak spawning season, providing fundamental insight into the importance of protecting the furthest upstream oyster reef as a sustained larval source to the downstream reefs. Thus, supporting the effectiveness of using field measurements for the validation of ABMs and subsequently using ABM simulations to bolster future field studies. Ultimately, this study provides an effective, generally applicable, approach to model larval ecology for restoration purposes.

Key words: ABM Lab, agent-based model, Caloosahatchee River Estuary, larval transport and dispersal, MIKE ECO Lab template, population connectivity

Implications for Practice

- A novel approach to study oyster larval transport and dispersal within the Caloosahatchee River Estuary and the broader Charlotte Harbor estuarine system was performed using an agent-based model (ABM).
- The ABM incorporates agent (oyster larvae) settlement behavior and salinity-related tolerances and mortality which, when validated with existing field data, provides insight into an upstream oyster reef as a vital larval source.
- This study was able to develop a working, generally applicable modeling framework serving as the foundation for future modeling and field-based studies focused on oyster reef restoration.

Introduction

Oyster reefs have declined in many estuarine and coastal ecosystems from overharvesting, diseases, and deteriorated water quality (Beck et al. 2011). The once-flourishing Chesapeake Bay oyster population has been reduced to 1% of its historical abundance from a myriad of issues (Rothschild et al. 1994). In 2012, Florida's Apalachicola Bay, a region producing 10% of the U.S. annual oyster harvest, experienced an oyster fishery

collapse attributed to low juvenile survival in the years prior to the collapse (Pine III et al. 2015). Although the Caloosahatchee River Estuary (hereinafter CRE) does not support a commercial oyster fishery, the estuary's oyster reefs are valued ecosystem components (Chamberlain & Doering 1998; Barnes et al. 2007).

Historically, the CRE (Fig. 1 cross-hatch region) located in Southwest Florida supported extensive *Crassostrea virginica* (Eastern oyster) reefs; however, oyster reef removal and man-made alterations to the estuary's hydrology have reduced the oyster population (Chamberlain & Doering 1998). Presently,
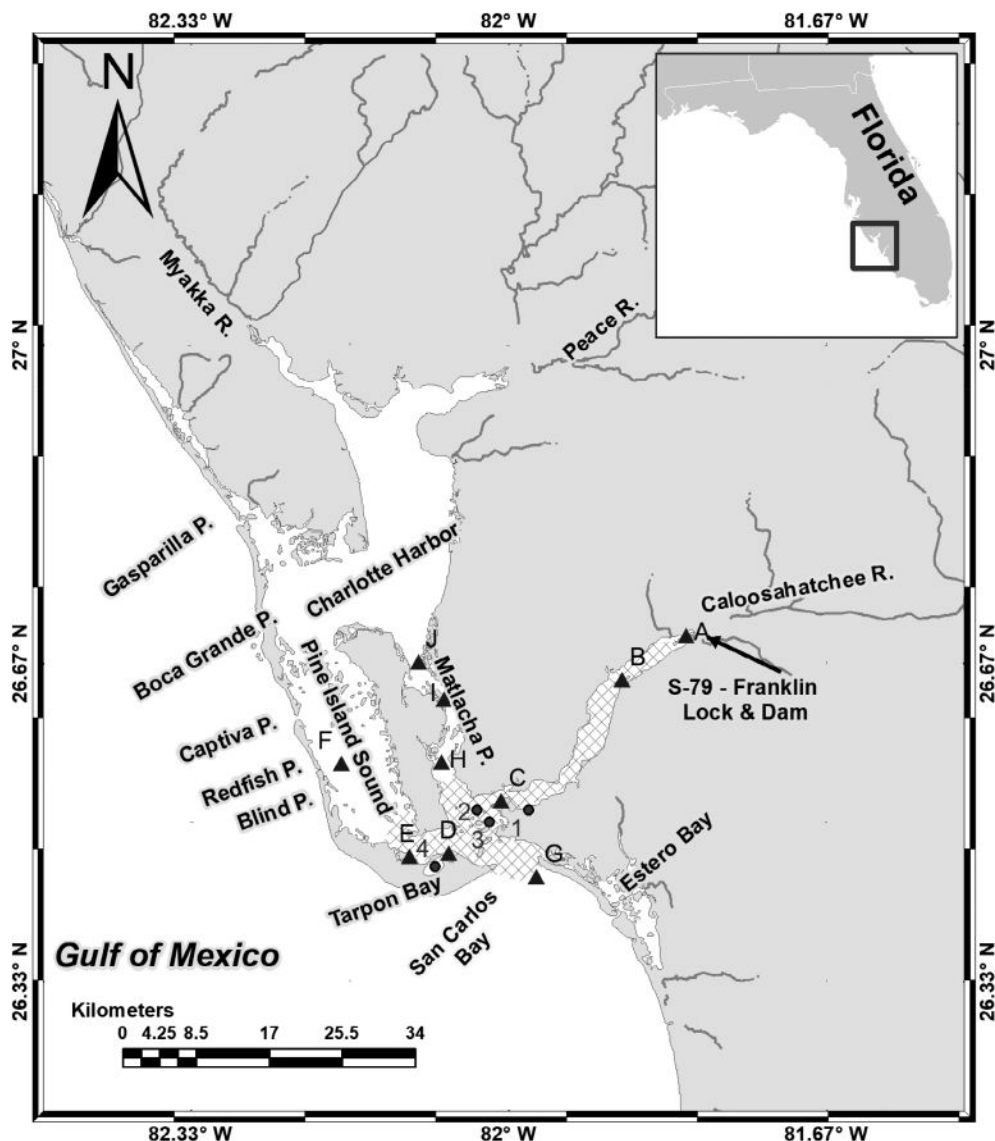
Figure 1. Map of the Charlotte Harbor estuarine system (CHES) study area showing the Caloosahatchee River Estuary (CRE) (cross-hatch region), oyster reef monitoring sites and agent release locations (1–4), and water quality monitoring stations (A–J).

CRE oysters experience vastly differing freshwater inflow depending on the season as Florida's subtropical climate produces wet (June to October) and dry (November to May) seasonal patterns. In addition, a lock and dam structure (S-79) controls 70% of the freshwater entering the estuary (Sun et al. 2016). Typically, freshwater releases from the dam are minimal during the dry season. In contrast, the estuary can be driven fresh by high inflow throughout the wet season (Chamberlain & Doering 1998) coinciding with the oyster's spawning period (late spring to early fall; Volety et al. 2015). Therefore, large pulsed and or sustained inflow may result in larval mortality, downstream larval flushing, and/or larvae flushed entirely out of the estuary (Chamberlain & Doering 1998; Volety et al. 2015).

Prior studies have been conducted within the estuary regarding inflow, oyster health, and habitat. Altered hydrology, including the unnaturally high and low inflow, has been identified as the key ecological stressor within the CRE (Barnes 2005). Barnes (2005) identified additional key CRE stressors (estuarine salinity, inflow, nutrient inputs, and physical alterations), which were implemented into a CRE habitat suitability index model (HSI). The HSI study by Barnes et al. (2007) found preferred inflow conditions (i.e. seasonally managed frequency distribution of inflow) and storing excess inflow in a constructed reservoir would provide more suitable habitat conditions than existing conditions without management. Volety et al. (2009) labeled the CRE oyster population at stage "caution" by accounting for biological responses (e.g. oyster density, larval recruitment, disease prevalence) and the estuary's hydrological

conditions (temperature and salinity). Buzzelli et al. (2013) simulated potential oyster densities resulting from varying inflow thereby providing a range of inflow to promote healthy oyster densities. However, agent-based modeling (ABM) of oyster larval transport (larval movement between two locations), considering the behavioral aspects of the agents (larvae), and dispersal (spread of larvae from spawning source to settlement site; Pineda et al. 2007) has not been conducted for the CRE and was recommended by Volety et al. (2015) as an important future study to better understand the influence of inflow on CRE oyster populations.

Previous studies by Kim et al. (2010, 2013) in Mobile Bay, Alabama utilized a hydrodynamic and larval transport model along with field data to investigate Eastern oyster larval transport and dispersal patterns under both realistic and idealized physical transport scenarios. Those studies provided a better understanding of larval movement among Mobile Bay's various regions and associated oyster reefs, thus providing a management tool to aid in the development and implementation of oyster reef restoration strategies. The ability to predict larval transport and dispersal under different inflow conditions is critical to a highly managed system because interannual differences in inflow could shift the target for oyster reef restoration from upstream (dry years) to downstream (wet years). A system-wide approach should consider adult oyster suitability indicators such as salinity, reef elevation, food supply, and substrate availability (Barnes et al. 2007). Additional consideration is needed to determine reef connectivity and larval supply for restoring and maintaining estuarine oyster populations. The present study uses an ABM comprised of a hydrodynamic model of the Charlotte Harbor estuarine system (Dye et al. 2020) and an ecological modeling module (MIKE ECO Lab; DHI 2017) to simulate oyster larval transport and dispersal within the CRE and the larger, encompassing Charlotte Harbor estuarine system hereafter CHES (Fig. 1). MIKE ECO Lab is a process-based customizable ecosystem modeling tool widely used to study the transport, dispersal, as well as foraging traits of various organisms such as eelgrass, coral larvae, starfish, sea birds, and marine mammals (Tay et al. 2012; Elsäßer et al. 2013; Canal-Verges et al. 2014; Heinänen et al. 2018; Kuusemäe et al. 2018; Cavalcante et al. 2020). The MIKE ECO Lab model template created specifically for *C. virginica* oyster larvae was tested in its ability to simulate dispersal patterns observed in situ in the CRE. Furthermore, simulated model outputs were used to (1) establish the connectivity patterns between the monitored oyster reef sites and (2) determine larval transport within the CHES.

Methods

Site Description

The CHES is a large (approximately 700–800 km^2), shallow, subtropical estuary located in Southwest Florida with an average microtidal range of 0.6 m (Scarlatos 1988). Marine water from the Gulf of Mexico enters the estuary through various inlets (e.g. Gasparilla Pass, Boca Grande Pass, Captiva Pass, Redfish Pass, Blind Pass, San Carlos Bay; Fig. 1) between the barrier

islands as well as San Carlos Bay. Freshwater enters the CHES by precipitation, watershed run-off, and three rivers; Myakka and Peace Rivers supply the northern portion while the Caloosahatchee River supplies freshwater to the southern region.

Located in the southern region of the CHES, the CRE (Fig. 1 cross-hatch region) has depths ranging from 0.3 to 6.0 m (1.5-m mean depth; Scarlatos 1988). Various man-made changes have altered the morphology and hydrology of the CRE. In the late 1800s, the Caloosahatchee River was artificially connected to Lake Okeechobee (Flaig et al. 1998). Modifications continued as the Caloosahatchee River, originally a meandering river, were straighten and deepened, and three lock and dam structures were constructed to improve flood control measures of Lake Okeechobee (Sun et al. 2016). Additionally, the furthest downstream lock and dam (S-79) acts as a salinity barrier between the fresh river water and the estuary's brackish water (Chamberlain & Doering 1998; Sun et al. 2016). The CHES is unique because of the more natural conditions in the northern region as compared to the very unnatural, man-made conditions in the CRE portion of the system.

The Model

This ABM presented in this study was built in ABM Lab, the Lagrangian module available in MIKE ECO Lab (DHI 2017), in order to describe Eastern oyster, *C. virginica*, larval transport within the CHES and more specifically larval transport and dispersal within the CRE (Fig. 1 cross-hatch region). The Eulerian–Lagrangian modeling framework applied in this study consists of a MIKE 21 hydrodynamic flexible mesh model (HD) (DHI 2017) integrated with the MIKE ECO Lab (DHI 2017) ecological modeling module. The HD uses a finite volume method to solve shallow water, depth-integrated incompressible Reynolds averaged Navier–Stokes Equations (DHI 2017). The MIKE ECO Lab module provides a customizable model template for users to develop mathematical equations and descriptions of target species, including their behavioral tendencies, and the environmental parameters (e.g. state variables, constants, forcing). The physical environment was simulated by the HD and the Eastern oyster-specific mathematical equations and descriptions were customized in the MIKE ECO Lab template for the study area. The movement and environmental interaction of simulated oyster larvae, hereinafter referred to as agents, were modeled by the overarching ABM.

The model description follows the ODD (Overview, Design concepts, Details) protocol (Grimm et al. 2006, 2010) for describing individual and ABMs developed "to standardize published model descriptions in order to make descriptions more understandable and complete."

Purpose. This ABM was developed to test the model's ability to numerically simulate measured Eastern oyster larval settlement at four monitored oyster reef sites within the CRE.

Entities, State Variables, and Scales. Four groups of agents are simulated with each group representing one of the four

oyster reef locations (Fig. 1, 1–4; please see section Field Data—In Situ Oyster and Larval Characteristics for description of reefs). Individuals of each group are characterized by their release site (1–4), position (x, y, z coordinates), and settlement status (i.e. settled or not settled onto sites 1–4).

An existing HD model of the CHES (Dye et al. 2020) generated the physical environment (time series of two-dimensional current vectors, surface water elevations, fluxes) for the ABM under the forcing of realistic wind, tide, and inflow. The HD spatial domain encompasses the entire CHES, all major tributaries, and extends 80 km offshore into the Gulf of Mexico (Fig. 2A). The HD accurately simulates the system's water levels, tidal heights, and flow dynamics and has been used to study the circulation dynamics as well as the effect of inflow and wind on neutrally buoyant simulated particles within the system (Dye et al. 2020). The HD's flexible triangular mesh (FM) (DHI 2017) resolution is approximately 250 m within the focus area of the study (CRE), approximately 700 m in the surrounding estuarine regions, and increases to 2.7 km at the outer boundary (Fig. 2A & 2B). A more detailed model description is provided in Dye et al. 2020.

Salinity was included in the ABM by interpolating in situ salinity data from six stations, which are part of the RECON monitoring system (http://recon.sccf.org/) (Fig. 1A–1G) and three gages deployed and maintained by the Charlotte Harbor Aquatic Preserve in Matlacha Pass (Fig. 1H–1J). Long-term salinity data were collected at each environmental monitoring site within the study area (Table S1; Fig. 1A–1J) and interpolated (distance weighted) into a high-resolution grid for the model domain, grid resolution of approximately 200 m (Fig. 2C). Hourly salinity values were extracted using the DHI MATLAB Toolbox (https://github.com/DHI/DHI-MATLAB-Toolbox/blob/master/Documentation/DHI_MATLAB_Toolbox_User_Guide.pdf). The resulting two-dimensional grids were converted into dfs2 file format and subsequently converted into a MIKE ECO Lab compatible file.

Process Overview and Scheduling. The simulation was executed with an 8-second time step in the following order: hydrodynamics, advection-dispersion, salinity, agent sensitivity to salinity (discussed in section Sensing), agent movement (x, y, z), and agent settlement behavior (discussed in section Basic Principles).

Design Concepts. *Basic Principles.* Agents were released in the model domain from the sites (Fig. 1, 1–4) found to be spawning during the study period (please see sections Field Data and Simulation for further description). Every agent is considered a successfully fertilized zygote and therefore capable of developing into a competent larva. During the simulation, every agent becomes competent (i.e. larvae has metamorphosed into the pediveliger stage thereby developing a foot to search for and subsequently attach [settle] onto hard substrate [Wallace et al. 2008]) to settle if the agent survives beyond the development period (Table 1).

Four requirements must be fulfilled for an agent to successfully settle onto a mesh grid cell classified as a settlement substrate (Fig. 1, 1–4). (1) An agent has developed and gained competency; (2) an agent's x, y coordinates in a given model time step coincide with a settlement substrate; (3) the agent is less than 0.5 m away from the settlement substrate; and (4) the current velocity must be less than 1.0 m/s at the time step of settlement (Table 1). Once agents settle onto a settlement substrate, the agents are considered successfully settled and are no longer subjected to any mortality, natural or salinity-based (please see sections Sensing and Stochasticity for further details).

Agent transport is regulated by current direction and velocities—both horizontal and depth-averaged vertical velocities—as well as settling velocities assigned to agents (Table 1). During the development period, an agent is assigned a neutral buoyancy with a settling speed of 0 m/s. Once an agent has progressed through the development period and is thereby competent to settle, an agent is assigned a settling speed of 0.007 m/s (Table 1).

Adaptation. After gaining competency, an agent will actively swim toward the benthic zone in a settlement attempt if the
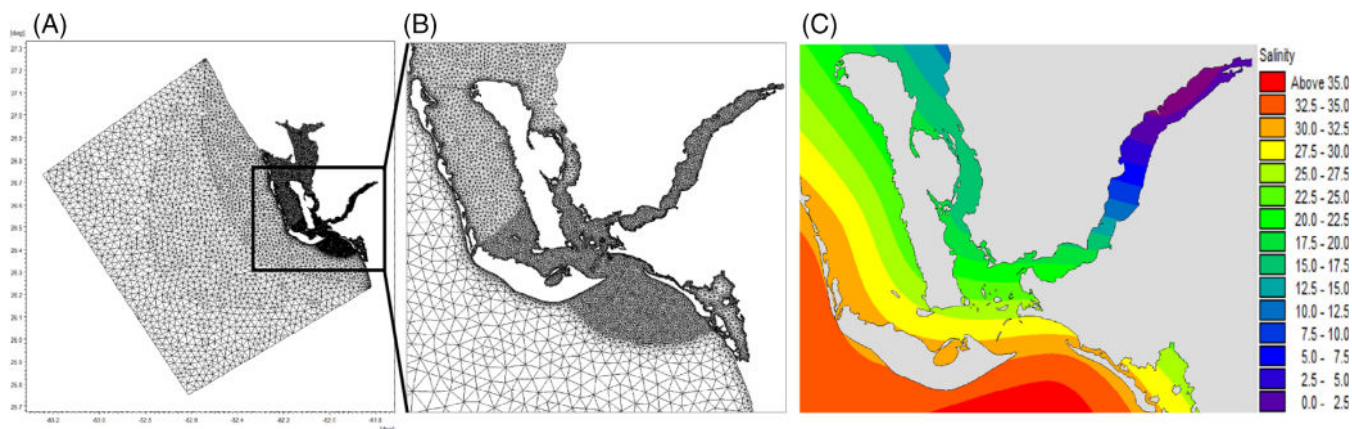

Figure 2. The hydrodynamic model (HD) computational mesh (A), zoomed-in view of the Caloosahatchee River Estuary (CRE) (B), and two-dimensional depth-averaged salinity grid (C).

Table 1. Mathematical formulations of the oyster larval agent-based model including functions, parameters, constants, and forcing. VTS refers to varying in time and space.

Function/Parameter/Constant	Value	Unit	Equation/References	
Age-dependent decreasing Weibull function mimicking Type III survivorship curve	—	—	$f(x) = \frac{\gamma}{\alpha}\left(\frac{x-\mu}{\alpha}\right)^{\gamma-1}\exp\left(-\left(\frac{x-\mu}{\alpha}\right)^{\gamma}\right)$	Pinder et al. 1978
Shape parameter of the survivorship curve (γ)	0.75	—	Rumrill 1990; Crockett et al. 2012; user defined	
Scale parameter of the survivorship curve (α)	0.1	—	Rumrill 1990; Crockett et al. 2012; user defined	
Minimum daily instantaneous mortality rate	0.01	day^{-1}	Rumrill 1990; user defined	
Maximum daily instantaneous mortality rate	0.12	day^{-1}	Rumrill 1990; user defined	
Development period before agent becomes competent to settle	10	days	$T_{larvae} = 110.79 \times \exp(-0.0825 \times T_w)$ T_w = water temperature°C T_{larvae} = larval period (in days)	Kennedy 1996; Table S1—water temperature°C
Settling speed—development period	0	m/s	Kim et al. 2010	
Settling speed—post-development period	0.007	m/s	Hidu & Haskin 1978; Kim et al. 2010	
Maximum planktonic larval (agent) duration	25	days	Kennedy 1996; Narváez et al. 2012	
Maximum distance from agent to suitable settlement substrate (site) for settlement	0.5	m	Cavalcante et al. 2020	
Minimum water depth at which at agent can settle	0.01	m	Volety et al. 2015; user defined	
Maximum water depth at which at agent can settle	4.0	m	Volety et al. 2015; user defined	
Maximum current speed for agent settlement	1.0	m/s	Cavalcante et al. 2020; user defined	

Forcing	Value	Unit	References
Horizontal current direction (HD)	VTS	Degrees	Data extracted from Dye et al. 2020 HD
Horizontal current speed (HD)	VTS	m/s	Data extracted from Dye et al. 2020 HD
Vertical current speed (HD)	VTS	m/s	Data extracted from Dye et al. 2020 HD
Water Elevation (HD)	VTS	m	Data extracted from Dye et al. 2020 HD
Horizontal dispersion	1.0	scaled eddy viscosity formulation	DHI 2017; Cavalcante et al. 2020; user defined
Salinity	VTS	PSU	See Table S1

agent, in its current simulation time step, is located within a model mesh cell designated as settlement substrate (Fig. 1, 1–4).

Sensing. Specific salinity tolerance ranges for agents and the complementing time durations were included in the MIKE ECO Lab template (Table 2). Agent salinity tolerance ranges (Davis 1958; Davis & Calabrese 1964) provide the lower threshold of salinity values before salinity timers are initiated. The required durations that agents must spend above each salinity threshold to reset the duration timer were user-defined; however, durations were largely based on the study by Kinne and Kinne (1962). If the salinity duration timer for an individual agent exceeds the maximum time in the corresponding salinity range (Table 2), the agent is classified as dead and removed from the simulation.

Stochasticity. A constant horizontal dispersion value, based on hydrodynamic model resolution, was assigned throughout the model domain (Table 1) because of the importance of horizontal dispersion (i.e. transport from non-resolved turbulence or eddies in numerical models) in coastal and estuarine environments (Geyer & Signell 1992). No vertical dispersion was included in the template. Considering the shallow nature of the study area, it is safe to assume that horizontal dispersion is the primary mode of agent transport (Suara et al. 2017). Additionally, particle resuspension was activated in the ABM which forces agents

contacting the benthic substrate back into resuspension unless the agents have settled onto a suitable substrate.

To reduce the overestimation of agent survival (Connolly & Baird 2010; Tay et al. 2012), natural mortality, beginning at the time of agent release, was included by an age-dependent decreasing Weibull function mimicking a type III survivorship curve (Pinder et al. 1978; Table 1).

Collectives. One individual collective of agents is assigned to each of the four sites. No differences exist between the collectives apart from their release location from one of the four sites. All state variables and traits are consistent for all agents within the simulation, regardless of collective.

Observations. Outputs obtained from the model include agent location (x, y), total surviving (i.e. nonsettled agents remaining in simulation) agents, and agent settlement assessed at each site (1–4). Outputs were saved every 1 hour; however, only outputs at the final time step (conclusion of simulation) were used to determine transport patterns and for further comparison with field data collected from the study area.

Initialization. Two thousand and five hundred agents were released from the individual sites during the 25-day simulations, thus representing a typical larval duration (Kennedy 1996; Narváez et al. 2012). Natural variability as well as uncertainty

Table 2. Mathematical formulations of the eastern oyster (*C. virginica*) larval agent-based model salinity tolerance ranges. SALDUR(1,2,3) refers to maximum time before mortality (days); saldur_thres(1,2,3) refers to salinity tolerance range (PSU);OYS refers to "particle classes" in ECOLab template.

Salinity tolerance range (PSU)	Equation	Maximum time before mortality (days)	References	Salinity rejuvenation timer (days)	References
7.5–10	IF SALDUR1/24 > saldur_thres1 THEN REMOVE {(OYS, 1)} ELSE 0	7	Davis 1958; Davis & Calabrese 1964	1	Kinne & Kinne 1962; user defined
5.0–7.5	IF SALDUR2/24 > saldur_thres2 THEN REMOVE {(OYS, 1)} ELSE 0	2	Davis 1958; Davis & Calabrese 1964	1	Kinne & Kinne 1962; user defined
<5.0	IF SALDUR3/24 > saldur_thres3 THEN REMOVE {(OYS, 1)} ELSE 0	0.25	Davis 1958; Davis & Calabrese 1964	1	Kinne & Kinne 1962; user defined

Table 3. Model sensitivity testing performed with the August 2011 simulation comparing the relative percentage of total and individual site settlement.

Site	2,500 Agents	Settlement (%)	5,000 Agents	Settlement (%)	10,000 Agents	Settlement (%)
1	6	0.24	4	0.08	17	0.17
2	72	2.88	121	2.42	236	2.36
3	99	3.96	178	3.56	313	3.13
4	4	0.16	7	0.14	16	0.16
Total	181	7.24	310	6.20	582	5.82

Table 4. Model simulation periods, locations, and number of agents released.

Year	Simulation Period	Agent Sources	Total Amount of Agents Released
2011	5–30 July	Sites 1 and 3	5,000
	5–30 August	Sites 1 and 3	5,000
	5–30 September	Sites 1, 2, and 3	7,500

Table 5. Percent agent survival (agents in the water column + settled) and agent settlement at the end of each simulation period and freshwater inflow at S-79 during the simulation period.

Year	Simulation Period	Agent Survival (%)	Agent Settlement (%)	Inflow Min–Max; Mean ± SD (m^3/s)
2011	1–30 July	13.4	1.2	5.7–59.5; 30.9 ± 14.1
	1–30 August	15.8	3.6	12.7–84.6; 48.4 ± 18.3
	1–30 September	14.8	2.0	12.7–135.1; 45.6 ± 30.2

exists in the literature regarding the specific values chosen to represent the larval characteristics (e.g. larval salinity tolerance ranges) (Tay et al. 2012). Therefore, all values (Tables 1 & 2) were kept constant throughout each simulation to normalize comparisons between the different simulations.

Input Data. Forcing of this ABM model was obtained from the HD (water levels, current velocities, and direction; Dye et al. 2020) and the two-dimensional depth-averaged salinity grids (Table 1).

Sensitivity Analysis

Since it was unknown how many larvae were released at each site during the spawning periods, model sensitivity to the number of agents released was tested. The sensitivity analysis provided an understanding of any difference between larval recruitment success and number of larvae (agents) released. Sensitivity analysis was performed for August 2011 by releasing 2,500, 5,000, or 10,000 agents from sites 1 and 3 in three separate simulations. The relative percentage of agent settlement at sites 1–4 was compared to determine any relative variability between simulations. Differences in percent total
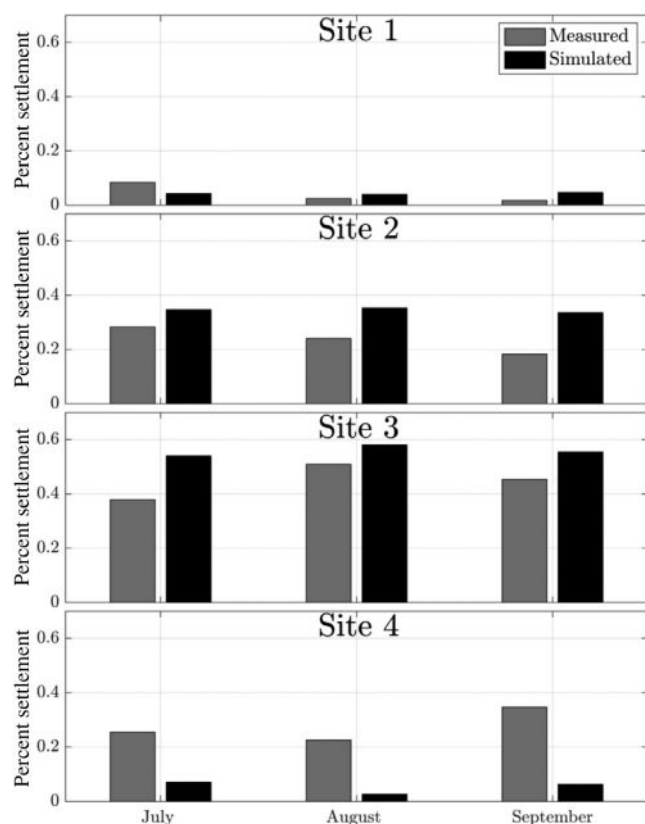
Figure 3. Percentage of monthly settlement measured (gray bars) and simulated (black bars) at sites 1–4. Calculated by (specific monthly settlement [simulated or measured] at a specific site/total specific monthly settlement [simulated or measured] at all sites) × 100.
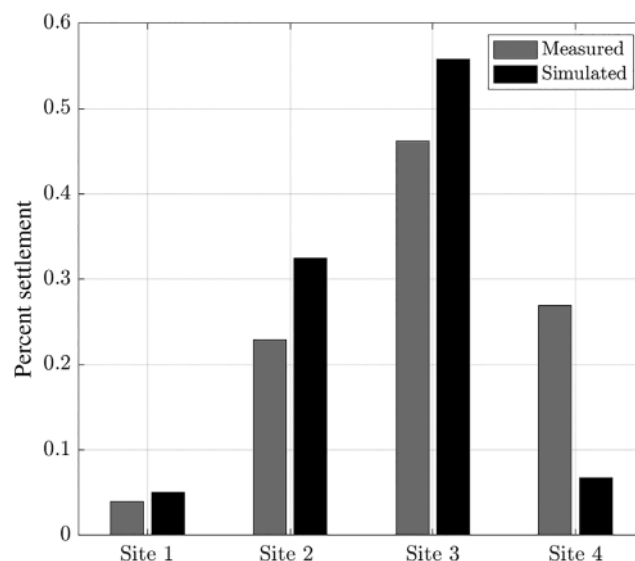

Figure 4. Percentage of total settlement measured (gray bars) and simulated (black bars) at sites 1–4. Calculated by (total settlement from each [simulation or measurement] at a specific site/total settlement from each [simulation or measurement] at all sites) × 100.

settlement at the four sites consisted of 1.04% between simulations releasing 2,500 and 5,000 and 0.38% between simulations releasing 5,000 and 10,000 agents (Table 3). This decreasing trend in the percentage of settlement with greater amounts of agents released occurred at sites 2 and 3 with less than 0.46% differences in percent settlement between simulations (Table 3). At sites 1 and 4, settlement percentage was lowest during the 5,000 agent release simulations. Minor differences in percent settlement of 0.02% occurred between simulations at site 4 while greater differences of 0.16% resulted between simulations at site 1 (Table 3). Sensitivity analysis provided evidence that greater amounts of agents released did not drastically enhance settlement and differences can be partially attributed to randomness in the stochastic processes of both dispersion and particle process descriptions. Therefore, it was decided to release 2,500 agents at the respective sites in each simulation.

Field Data—In Situ Oyster and Larval Characteristics

A long-term (2000–2016) oyster monitoring study was performed by Volety et al. (2015) at four oyster reef sites (Fig. 1, 1–4) along the CRE's salinity gradient. Site 1 marks the farthest upstream extent of living oysters, and sites 2–4 are situated progressively downstream within increasingly higher salinity regimes. Live oyster density is generally high, exceeding 800 oysters/m^2 at all sites except at site 1 during years of extremely high inflow. Adult oysters are reproductively active in the summer months (May to October) with larval settlement subsequently peaking (June to November) and correlated with inflow (i.e. reduced settlement with high inflow; Volety et al. 2015). The 2011 field season provided larval settlement and histological analysis data used in this study.

Larval settlement was evaluated monthly from the four sites by deploying three shell strings suspended within the water column, approximately 10–15 cm above the bottom of the estuary. Each shell string consisted of 12 oyster shells with shell heights of about 5.0–7.5 cm, stacked inner shell surface-oriented downwards, and suspended by galvanized wire via polyvinyl chloride (PVC) poles (Volety et al. 2015). Field measurements of larval settlement were compared with simulated settlement to test the model's ability to accurately reproduce the measured settlement patterns.

Histological analysis was performed to determine the reproductive state of oysters within the estuary using methods by Fisher et al. (1996) and the International Mussel Watch Program (1980). Each month, 10 oysters were collected, analyzed, and assigned a value ranging from 1 to 5 indicating the oyster's gonadal condition. Gonad index values ranging from 4 to 5 were classified as oyster spawning events and subsequently used to determine from which site to release agents within the model simulations.

ABM Simulations

Individual model simulations were performed for the months of July, August, and September 2011 with monthly simulation
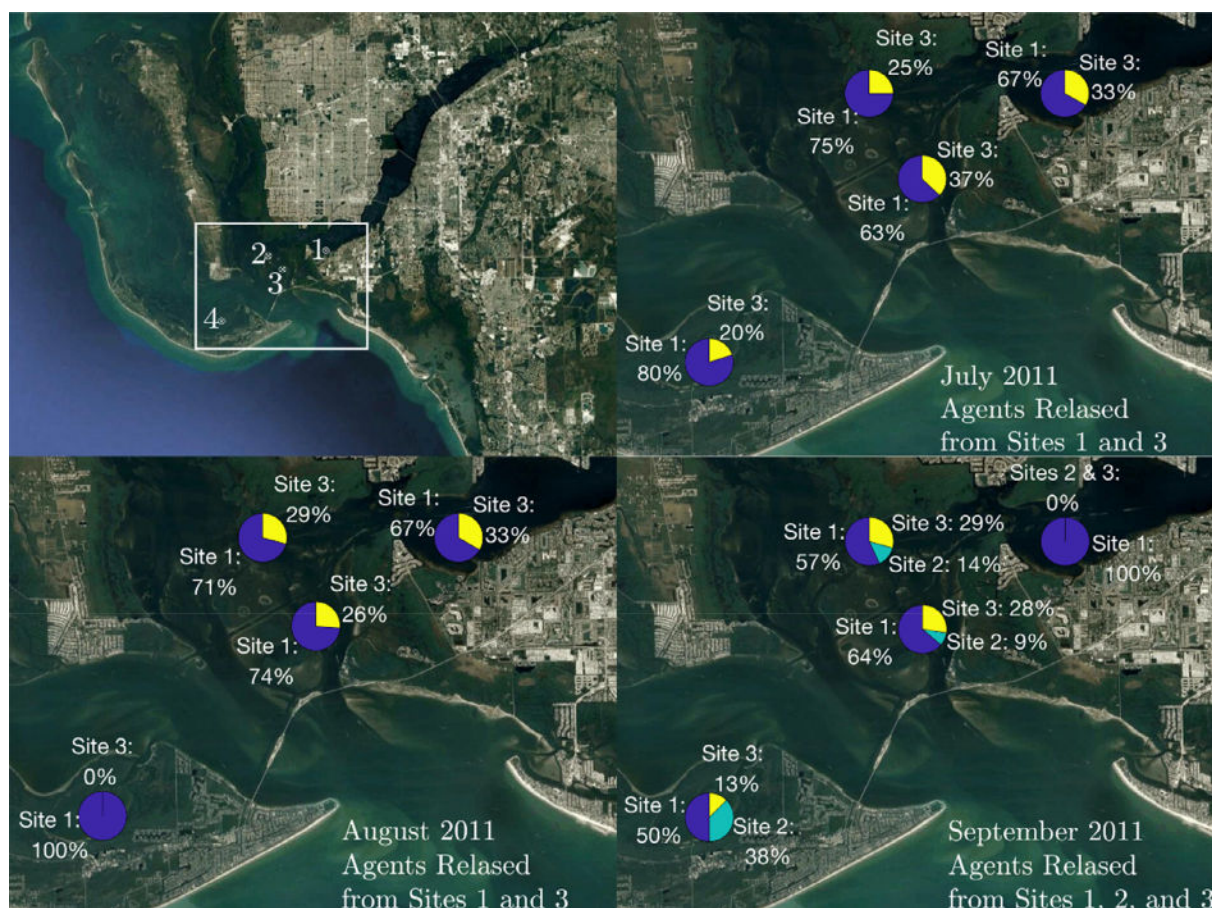
Figure 5. Connectivity between the four oyster reefs (numbers 1–4 in the top left map) established from July, August, and September 2011 simulations. The different colored sectors represent the percentage of agents settled at each site, respectively, released at sites 1 (purple), 2 (yellow), and 3 (blue-green).

periods coinciding with observed site-specific spawning (Table 4). Agents were released synchronously on the fifth of each simulation month, 1 hour after the larger high tide, during the ebbing tide. Uncertainty in the timing of oyster spawning resulted in the decision to release agents on the ebbing tidal phase as it would provide the "worst case scenario" for larval retention within the estuarine system.

Field measurements determining site-specific spawning by means of histological analysis were conducted within the first week of each month. The model release date (fifth of each month) was chosen to standardize the simulations and reduce field measurement bias as much as possible. Two thousand and five hundred agents were released from the individual sites (Table 4; Fig. 1, 1–3) indicated by the field observations to be spawning based on the gonad index values. The simulations were conducted for 25 days to represent a typical planktonic larval phase (Kennedy 1996; Narváez et al. 2012).

Comparison of Simulated and Observed Larval Settlement within the CRE

In situ oyster settlement measurements (see section Field Observations—In Situ Oyster and Larval Characteristics) were compared to the simulated settlement to test model performance in predicting observed settlement. However, simulated settlement does not account for post-larval settlement mortality (Osman et al. 1989; Narváez et al. 2012) and cannot be directly compared to the observed measurements in terms of magnitude. Therefore, comparisons between simulated and observed settlement are in terms of trends, an ecologically viable method used by Narváez et al. (2012), with differences indicating the potential importance of post-settlement mortality.

Variability existed between element sizes of the hydrodynamic model's triangular mesh, which serves as the available settlement substate at the sites (1–4). Therefore, to normalize the simulated settlement data, the total simulated larval settlement at each site were divided by the site's settlement area (m^2 grid size) to calculate a settlement/m^2 value (e.g. settlement density).

Results

Percentage of Agent Survival and Settlement

The percentage of agent survival at the end of each simulation period was calculated ([settled + nonsettled agents/total # of

agents released] × 100). Agent survival ranged from 13 to 16% with lowest survival during the July simulation and highest survival subsequently in August (Table 5).

The percentage of agent settlement for each simulation was additionally calculated ([total settled/total # of agents released] × 100; Table 5). Variability in the percentage of settlement existed between the simulated months. The July simulation experienced the lowest settlement success with 1.2% of released agents successfully settling. Agents experienced the greatest settlement of 3.6% during August, while the September simulation had a settlement of 2.0%.

Comparison of Simulated and Measured Settlement

Figure 3 displays settlement percentage comparisons between the measured (min = 3.3%, max = 47.0%) and simulated (min = 4.3%, max = 56.3%) settlement at each site for the individual monthly simulations. The pattern of increased measured settlement from sites 1 to 3 followed by a reduction at site 4 is reflected in the simulated data. In July, measured and simulated percentages at sites 1 and 2 differed by less than 6.3%, while greater differences (18.3%) were found at sites 3 and 4. August and September display similar trends between measured and simulated settlement as July; however, with closer matches at sites 1 and 3 as compared to sites 1 and 2 in July (Fig. 3). Generally, the overall simulated settlement was greater than the measured settlement at sites 1–3; however, measured settlement was always greater at site 4.

In order to test how well the ABM performs overall in simulating specific site settlement, comparisons between the percentage ([total settlement from each simulation at a specific site/total settlement from each simulation at all sites] × 100; e.g. [July + August + September settlement at site 1]/[July + August + September settlement at all sites] × 100) of total measured and simulated settlement at each individual site are presented in Figure 4. At site 1, both measured and simulated total settlement exhibit similar percentages. The measured and simulated settlement at sites 2 and 3 are within 11.2% of each other, with a lesser proportion of measured settlement at both sites. Although the simulated settlement is underestimated compared to the measured at site 4, a trend of increasing settlement from sites 1 to 3, followed by a reduction in settlement from site 3 to 4 is found in both measured and simulated settlement. The ability of the simulations to acceptably reproduce measured settlement allowed connectivity patterns between the sites to be examined.

Connectivity Patterns

Agents were released from sites 1 and 3 in the July 2011 simulation (Table 4). Self-recruitment dominated at site 1 with 67.0% of the total settlement being agents released from site 1 (Fig. 5). Similarly, total settlement of 75.0, 63.0, and 80.0% at the downstream sites 2–4, respectively, resulted from agents released from site 1 thus indicating downstream movement of agents (Fig. 5). Once again, agents were released from sites 1 and 3 in the August simulation (Table 4). The percentage of agent settlement in the August simulation was similar to the July
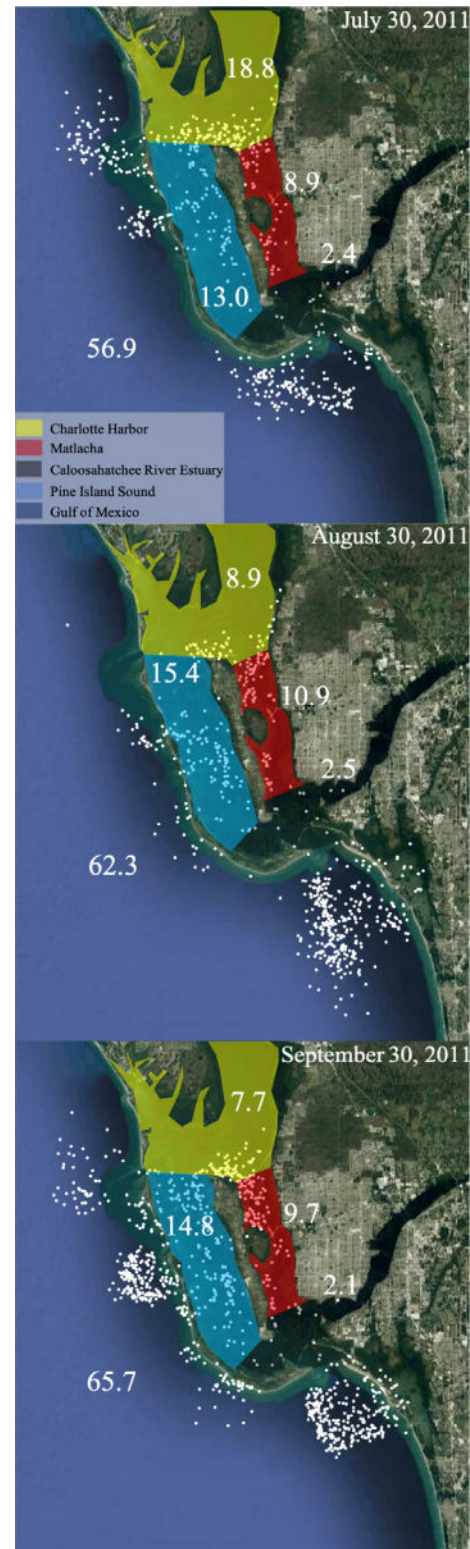

Figure 6. Distribution of agents (white circles) and percentage of agent surplus in each region (demarcated by colored areas) at the conclusion of each 2011 monthly simulation.

simulation except settlement at site 4 consisted entirely of agents released from site 1 (Fig. 5). In contrast to the other simulations, agents were released from sites 1, 2, and 3 in the September
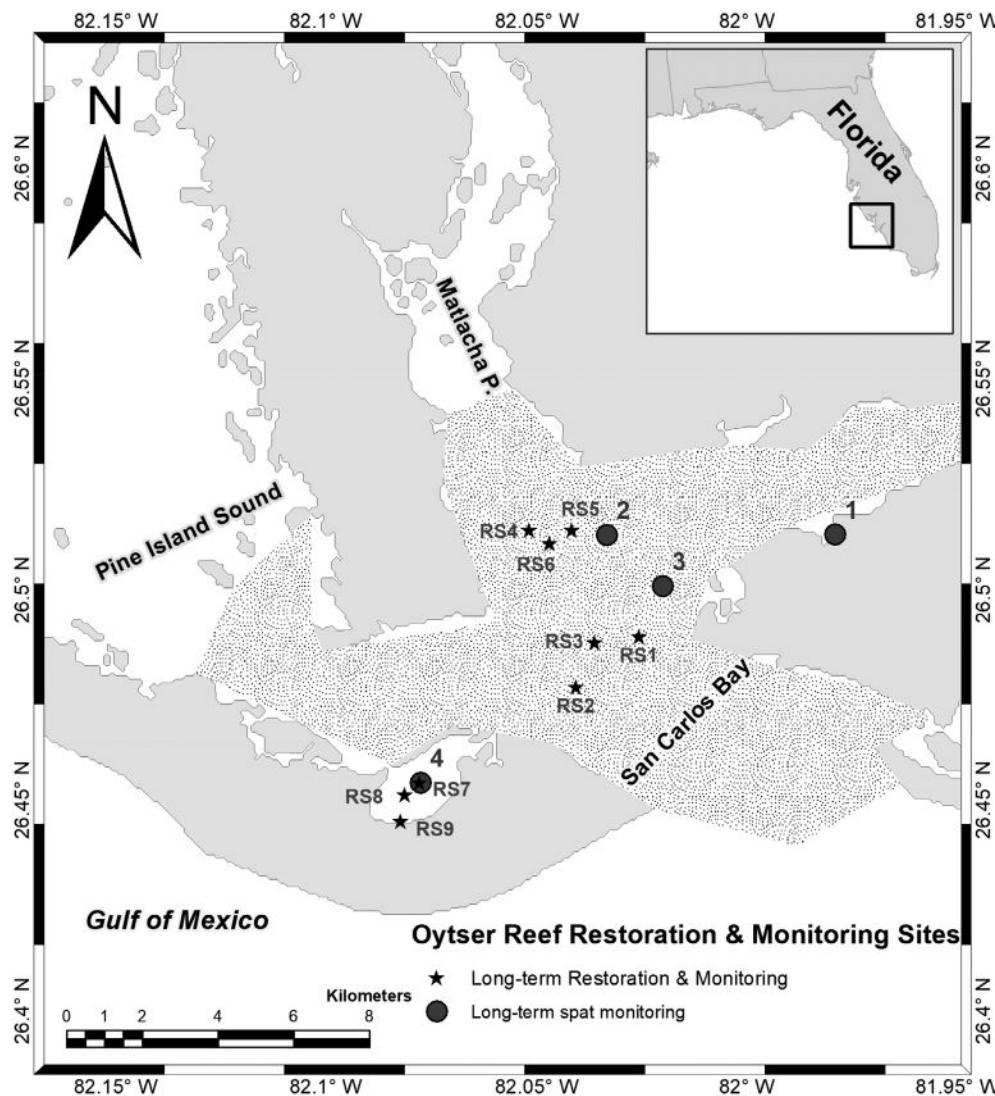
Figure 7. Oyster reef sites 2016–2020: Reference (RS1, 4, 7), restored (RS2, 5, 8), and control (RS3, 6, 9).

simulation (Table 4). Settlement at site 1 consisted entirely of self-recruited agents while settlement from site 1 agents progressively diminished moving downstream, as agents released from site 2 made up 14.0, 9.0, and 38.0% of total site settlement at sites 2–4, respectively. However, settlement at the downstream sites was still dominated (50–64%) by the downstream movement of agents released from site 1 (Fig. 5).

Agent Surplus

The present study termed "agent surplus" as nonsettled agents present at the completion of each simulation. Percentage of agent surplus was calculated in each region (identified by colored regions in Fig. 6) by dividing the number of agents in each region by the total number of agents remaining in the simulation. Overall, the percentage of agent surplus displayed similar trends between the three simulations, with the greatest variability

existing in the Charlotte Harbor and Gulf of Mexico regions. In each simulation, 56.9–65.7% of the agent surplus existed within the Gulf of Mexico (Fig. 6 dark blue) as agents were transported out of the system through various inlets. Pine Island Sound (Fig. 6 blue) and Matlacha Pass (Fig. 6 red) contained 13.0–15.4% and 8.9–10.9% of the total surplus, respectively (Fig. 6). Surplus in the CRE (Fig. 6 black) was consistently less than 2.5% (Fig. 6). Charlotte Harbor (Fig. 6 yellow) received 7.7 and 8.9% of the surplus in the August and September simulations, respectively, with 18.8% surplus in July (Fig. 6).

Oyster Reef Restoration

Oyster reef restoration efforts since 2016 have occurred throughout San Carlos Bay and Tarpon Bay with projects adding 10 cm washed fossil shell at elevations from −0.25 to −0.75 m National Geodetic Vertical Datum (NGVD). All of
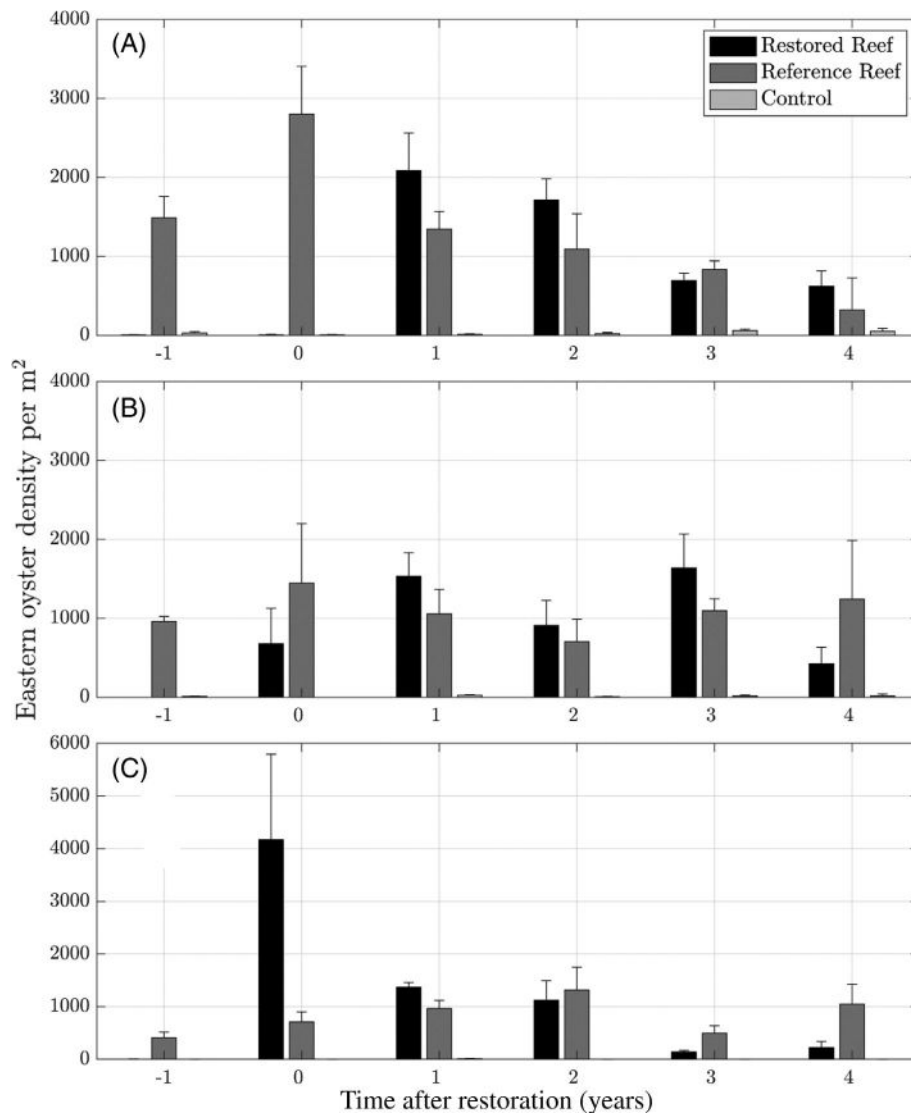
Figure 8. Eastern oyster (*Crassostrea virginica*) density and error bars indicating ± SE at restored, reference, and control sites. Please note the different *y*-axis values. (A) Upper San Carlos Bay, (B) lower San Carlos Bay, (C) Tarpon Bay. Fossil shell substrate was added to restored reefs at time = 0. Pre-construction monitoring at all sites occurred 1 year prior to construction (year = −1). Reference reefs are near restored reefs and are thought to represent healthy reefs. Control sites were at similar elevations to reference and restored reefs but had few live oysters.

the sites (Fig. 7, RS1-RS9) have exhibited recruitment and have exceeded the targeted live oyster densities greater than $100/m^2$ (Fig. 8 and Data S1 for more detailed description of oyster density calculation).

Discussion

The study's promising results serve as a proof of concept that this ABM model can be used as a viable tool for simulating oyster transport and dispersal dynamics, considering salinity stress and behavioral aspects of the agents (oyster larvae). Agent survival and settlement data show that greater settlement percentage resulted with greater agent survival, which was to be expected as a larger number of surviving agents would increase the chances of settlement. An in-depth analysis of the influence of inflow, salinity, and resulting agent survival and settlement is beyond the scope of this study. However, it is interesting to note that the lowest percentage of agent survival and settlement occurred in July, which also had the lowest minimum, maximum, and mean inflow as compared to the other simulation months; while the August simulation with the greatest agent survival and settlement percentages had the greatest mean inflow. It was expected that the simulation month with the greatest inflow (causing reduced salinity) would have resulted in the

lowest agent survival and subsequent settlement. However, these interesting and unexpected results warrant further investigation in a subsequent study.

Overall, the ABM presented in this study reproduced measured larval settlement at the four monitored sites within the estuarine system. The model recreated the measured settlement pattern of increasing settlement from sites 1 to 3 followed by a reduction in settlement at site 4. Additionally, although the model generally (apart from site 4) overpredicted settlement (at most by 21.5%) at the individual sites, there was still a reasonable agreement between the measured and simulated settlement. However, discrepancies did exist between the measured and simulated settlement, which could be attributed to inaccuracies introduced into the simulations by the chosen MIKE ECO Lab template parameters.

For example, the number of agents remaining at the completion of the simulations (calculated as percentage agent survival provides insight into the combined effects of natural and salinity-induced mortality. Natural mortality was incorporated into the simulations through the age-dependent decreasing Weibull function mimicking a type III survivorship curve Pinder et al. 1978). Nonetheless, the natural mortality parameters, based on *C. gigas* oyster larvae, may be over or underestimating natural mortality found in Gulf of Mexico *C. virginica* larvae. The variability in agent survival can also be attributed to salinity-related mortality based on salinity tolerance ranges of *C. virginica* oyster larvae from Chesapeake Bay and Long Island Sound because no tolerance studies were available for the Gulf of Mexico. The template could be improved through laboratory experiments to determine the specific CHES's larval salinity tolerances ranges in addition to more accurate information regarding natural mortality within the system. Furthermore, although the investigation of the influence of inflow, salinity, and resulting agent mortality is beyond the scope of this study; brief simulation analyses did not indicate a specific time period(s) within the simulations resulting in an abundance of instantaneous agent mortality. Rather the agents gradually suffered salinity-induced mortality and were removed from the simulation by low salinities associated with inflow.

Despite the differences between measured and simulated settlement, the reasonable comparison results provided the opportunity to determine connectivity patterns between the four sites. The simulated results provide strong supporting evidence to Volety et al.'s (2015) findings of site 1's role as an important larval source to the downstream sites (2–4) as well as the contributions sites 2 and 3 provide to each other. In summary, agents released from site 1 provided at least 50.0% of total settlement at the downstream sites. Additionally, even when agents were released from three sites as opposed to two, agents released from site 1 still provided at least 50.0% of the total settlement at the downstream sites. Site 1's furthest upstream location and importance as a larval source to the downstream sites could be cause for concern as its upstream location is likely more impacted by sustained inflow as compared to the other sites (Buzzelli et al. 2013).

Investigation of each simulation revealed four key agent transport patterns. (1) A cluster of agents is always transported in the southerly direction out of San Carlos Bay into the Gulf of Mexico, where the agents generally remain congregated outside of the bay and do not return into the system. (2) A portion of agents are transported from the CRE into Matlacha Pass and Pine Island Sound and remain or are further transported into northern Charlotte Harbor. (3) Agents are transported from the CRE through Matlacha Pass and Pine Island Sound into northern Charlotte Harbor, and then move through Boca Grande Pass out into the Gulf of Mexico. (4) Few agents, compared to the total amount released, remain in the CRE near the settlement sites approximately 12–20 days post-release. At the completion of the simulations, 56.9–65.7% of surviving, unsettled agents were transported into the Gulf of Mexico and therefore can be considered lost to the system as those agents generally did not move back into the system. However, the remaining 34.3–43.1% of unsettled agents remain within the system's various regions and represent an "agent surplus." This surplus has important oyster management and restoration implications by providing evidence that (1) a large portion of unsettled agents are retained within the system and (2) a greater abundance of settlement may have occurred if additional settlement sites were available; future work should include the mapping and monitoring of additional oyster reefs (i.e. simulation settlement sites), or identification of suitable areas for the creation or enhancement of reefs. For example, greater measured settlement occurred at site 4 possibly resulting from site 4's location in Tarpon Bay, a semi-enclosed bay and extension of San Carlos Bay, and because no agents were released from site 4 during any simulation (i.e. no measured spawning at site 4). However, additional oyster reefs exist within the bay which may have been spawning during the simulation period, therefore providing larvae to the neighboring sites not captured in the simulations. Expanding on the most recent oyster reef mapping efforts (https://geodata.myfwc.com/datasets/oyster-beds-in-florida?geometry=-82.094%2C26.504%2C-82.012%2C26.518) and monitoring additional oyster reefs within the CRE will hopefully close this knowledge gap and improve simulation results.

The ABM results provided dispersal patterns between field-measured oyster reef sites thus supporting evidence to previous field-based studies (Volety et al. 2015), insight into agent transport pathways, and resulting "agent surplus." Insights into transport pathways and "agent surplus" can aid in selecting locations to construct new oyster reefs as well as deciding which degraded oyster reefs show the greatest potential for successful restoration (Kim et al. 2013; Smyth et al. 2016; Arnold et al. 2017). This system-wide approach highlights the oyster reef connectivity and the relative value of specific reefs and restoration sites in relation to larval supply.

The restoration projects (Figs. 7-8) were planned using habitat suitability models for adult oysters and did not consider the supply and transport of larvae between existing and restored reefs. The results from this study will be applied to future restoration planning that seeks a system-wide approach considering

larval dispersal dynamics to improve site selection for future restoration efforts.

This ABM framework and study approach is an important tool for the restoration and management of oyster reefs and can be implemented in other estuaries. Hydrodynamic modeling of estuaries has greatly increased in the past decades (Brush & Harris 2010), therefore modeling outputs needed to force the ABM are likely available for most estuaries. The MIKE ECO Lab template can also be customized to an organism's estuary-specific biological characteristics (e.g. salinity tolerances of Chesapeake Bay oyster larvae). Ultimately, in situ field measurements (e.g. spawning periods, settlement) may be the limiting factor(s) to attempt a similar study, however alternative methods are possible. Water temperature measurements are generally available in most estuaries and can serve as a proxy for histological analysis to initiate spawning events in the simulations (i.e. agent release) (North et al. 2008; Kim et al. 2010). For example, Volety et al. (2015) found a range of annual spawning periods in the CRE lasting between 2 and 9 months depending on the oyster reef location and inflow, however active spawning closely followed seasonal water temperature periods greater than 21°C. Additionally, larval settlement collection and analysis may be too laborious. An alternative would be to collect bivalve larval concentrations at specific suitable settlement locations (i.e. oyster reefs) and compare field to simulated data with the assumption that upon reaching a suitable settlement location (i.e. oyster reef), the bivalve (agent) is classified as settled (Elsäßer et al. 2013). Alternatively, this modeling framework could first determine locations to implement a field monitoring program, subsequently using the field measurements to validate the simulated larval transport and dispersal.

The utility of using field measurements to validate ABMs and subsequently using ABM simulation results to pursue future field studies and restoration efforts (or vice versa) is an iterative process allowing managers and modelers to improve their restoration and research efforts continuously and collaboratively (Buzzelli et al. 2013). There are inherent positives and negatives associated with field and modeling studies, as some questions cannot be answered through field or modeling work alone. However, when used together, field and modeling studies can bolster one method's finding while introducing new findings and questions that may not have been previously considered or possible to identify (Ahn & Ronan 2020; Skogen et al. 2021).

Acknowledgments

LITERATURE CITED

Ahn JE, Ronan AD (2020) Development of a model to assess coastal ecosystem health using oysters as the indicator species. Estuarine, Coastal and Shelf Science 233:106528

Arnold WS, Meyers SD, Geiger SP, Luther ME, Narváez D, Frischer ME, Hofmann E (2017) Applying a coupled biophysical model to predict larval dispersal and source/sink relationships in a depleted metapopulation of the eastern oyster *Crassostrea virginica*. Journal of Shellfish Research 36: 101–118

Baggett LP, Powers SP, Brumbaugh RD, Coen LD, DeAngelis BM, Greene JK, Bushek D (2015) Guidelines for evaluating performance of oyster habitat restoration. Restoration Ecology 23:737–745

Barnes T (2005) Caloosahatchee Estuary conceptual ecological model. Wetlands 25:884–897

Barnes TK, Volety AK, Chartier K, Mazzotti FJ, Pearlstine L (2007) A habitat suitability index model for the eastern oyster (*Crassostrea virginica*), a tool for restoration of the Caloosahatchee Estuary, Florida. Journal of Shellfish Research 26:949–959

Beck MW, Brumbaugh RD, Airoldi L, Carranza A, Coen LD, Crawford C, et al. (2011) Oyster reefs at risk and recommendations for conservation, restoration, and management. Bioscience 61:107–116

Brush MJ, Harris LA (2010) Advances in modeling estuarine and coastal ecosystems: approaches, validation and applications. Ecological Modelling 221: 965–1088

Buzzelli C, Doering PH, Wan Y, Gorman P, Volety A (2013) Simulation of potential oyster density with variable freshwater inflow (1965–2000) to the Caloosahatchee River Estuary, Southwest Florida, USA. Environmental Management 52:981–994

Canal-Verges P, Potthoff M, Hansen FT, Holmboe N, Rasmussen EK, Flindt MR (2014) Eelgrass re-establishment in shallow estuaries is affected by drifting macroalgae–evaluated by agent-based modeling. Ecological Modelling 272:116–128

Cavalcante GH, Vieira F, Mortensen J, Ben-Hamadou R, Range P, Goergen E, Campos E, Riegl B (2020) Chapter Eight - Biophysical model of coral population connectivity in the Arabian/Persian Gulf. Advances in Marine Biology 87(1):193–221. https://doi.org/10.1016/bs.amb.2020.07.001

Chamberlain RH, Doering PH (1998) Freshwater inflow to the Caloosahatchee Estuary and the resource-based method for evaluation. Pages 274. In: Treat SF (ed) Proceedings of the Charlotte Harbor Public Conference and Technical Symposium. South Florida Water Management District, Punta Gorda, Florida

Connolly SR, Baird AH (2010) Estimating dispersal potential for marine larvae: dynamic models applied to scleractinian corals. Ecology 91:3572–3583

Crockett A, Delsouz A, DeGregorio J, Muhealden A, Streicher D (2012) Design and analysis of a sustainable oyster aquaculture business for the West and Rhode Rivers. IEEE Systems and Information Engineering Design Symposium, 112–117. https://ieeexplore.ieee.org/stamp/stamp.jsp?arnumber=6215123&casa_token=N2EQkxWalCgAAAAA:fN77T QjFboqGWD1Z6pfdmmeoP7bL8ErMRrtsKDnsjUPoVvwH7e1Nc2bcOL 4nBIzwUGt7luKSfg&tag=1

Davis HC (1958) Survival and growth of clam and oyster larvae at different salinities. The Biological Bulletin 114:296–307

Davis HC, Calabrese A (1964) Combined effects of temperature and salinity on development of eggs and growth of larvae of *M. mercenaria* and *C. virginica*. Fishery Bulletin 63:643–655

DHI Water and Environment (2017) Hydrodynamic Module User Guide. MIKE 21 Flow Model FM. Hørsholm, Denmark: DHI. https://manuals.mikepoweredbydhi.help/2017/Coast_and_Sea/MIKE_FM_HD_2D.pdf

DHI Water and Environment (2017) Numerical Lab for Ecological and Agent Based Modelling User Guide. MIKE ECO LAB. Hørsholm, Denmark: DHI. https://manuals.mikepoweredbydhi.help/2017/General/MIKE_ECO_Lab_UserGuide.pdf

Dye B, Jose F, Allahdadi MN (2020) Circulation dynamics and seasonal variability for the Charlotte Harbor estuary, Southwest Florida coast. Journal of Coastal Research 36:276–288

Elsäßer B, Fariñas-Franco JM, Wilson CD, Kregting L, Roberts D (2013) Identifying optimal sites for natural recovery and restoration of impacted biogenic habitats in a special area of conservation using hydrodynamic and habitat suitability modelling. Journal of Sea Research 77:11–21

Fisher WS, Winstead JT, Oliver LM, Edminston HL, Bailey GO (1996) Physiological variability of eastern oysters from Apalachicola Bay, Florida. Journal of Shellfish Research 15:543–555

Flaig EG, Srivastava P, Capece JC (1998) Analysis of water and nutrient budgets for the Caloosahatchee watershed – evaluation of available hydrological data for the Caloosahatchee watershed. *Southwest Florida Research and Education Center for SWMC*

Geyer WR, Signell RP (1992) A reassessment of the role of tidal dispersion in estuaries and bays. Estuaries 15:97–108

Grimm V, Berger U, Bastiansen F, Eliassen S, Ginot V, Giske J, Huth A (2006) A standard protocol for describing individual-based and agent-based models. Ecological Modelling 198:115–126

Grimm V, Berger U, DeAngelis DL, Polhill JG, Giske J, Railsback SF (2010) The ODD protocol: a review and first update. Ecological Modelling 221:2760–2768

Heinänen S, Chudzinska ME, Mortensen JB, Teo TZE, Utne KR, Sivle LD, Thomsen F (2018) Integrated modelling of Atlantic mackerel distribution patterns and movements: a template for dynamic impact assessments. Ecological Modelling 387:118–133

Hidu H, Haskin HH (1978) Swimming Speeds of Oyster Larvae Crassostrea virginica in Different Salinities and Temperatures. Estuaries, 1(4):252. https://doi.org/10.2307/1351527

International Mussel Watch (1980) Pages 248. National Academy of Sciences, Washington D.C: The National Academies Press. https://doi.org/10.17226/19786

Kennedy VS (1996) Biology of larvae and spat, in the eastern oyster: *Crassostrea virginica*. Pages 371–421. In: Kennedy VS, Newell RIE, Eble AF (eds) The eastern oyster, *Crassostrea virginica*. Maryland Sea Grant, College Park, Maryland

Kim CK, Park K, Powers SP, Graham WM, Bayha KM (2010) Oyster larval transport in coastal Alabama: dominance of physical transport over biological behavior in a shallow estuary. Journal of Geophysical Research 115:C10019

Kim CK, Park K, Powers SP (2013) Establishing restoration strategy of eastern oyster via a coupled biophysical transport model. Restoration Ecology 21:353–362

Kinne O, Kinne EM (1962) Rates of development in embryos of a cyprinodont fish exposed to different temperature–salinity–oxygen combinations. Canadian Journal of Zoology 40:231–253

Kuusemäe K, von Thenen M, Lange T, Rasmussen EK, Pothoff M, Sousa AI, Flindt MR (2018) Agent Based Modelling (ABM) of eelgrass (*Zostera marina*) seedbank dynamics in a shallow Danish estuary. Ecological Modelling 371:60–75

Narváez DA, Klinck JM, Powell EN, Hofmann EE, Wilkin J, Haidvogel DB (2012) Modeling the dispersal of eastern oyster (*Crassostrea virginica*) larvae in Delaware Bay. Journal of Marine Research 70:381–409

North EW, Schlag Z, Hood RR, Li M, Zhong L, Gross T, Kennedy VS (2008) Vertical swimming behavior influences the dispersal of simulated oyster larvae in a coupled particle-tracking and hydrodynamic model of Chesapeake Bay. Marine Ecology Progress Series 359:99–115

Osman RW, Whitlatch RB, Zajac RN (1989) Effects of resident species on recruitment into a community: larval settlement versus post-settlement mortality in the oyster *Crassostrea virginica*. Marine Ecology Progress Series 54:61–73

Pinder JE, Wiener JG, Smith MH (1978) The Weibull distribution: a new method of summarizing survivorship data. Ecology 59:175–179

Pine WE III, Walters CJ, Camp EV, Bouchillon R, Ahrens R, Sturmer L, Berrigan ME (2015) The curious case of eastern oyster *Crassostrea virginica* stock status in Apalachicola Bay, Florida. Ecology and Society 20:46

Pineda J, Hare JA, Sponaugle S (2007) Larval transport and dispersal in the coastal ocean and consequences for population connectivity. Oceanography 20:22–39

Rothschild B, Ault J, Goulletquer P, Héral M (1994) Decline of the Chesapeake Bay oyster population: a century of habitat destruction and overfishing. Marine Ecology Progress Series 111:29–39

Rumrill S (1990) Natural mortality of marine invertebrate larvae. Ophelia, 32(1-2):163–198. http://dx.doi.org/10.1080/00785236.1990.10422030.

Scarlatos PD (1988) Caloosahatchee estuary dynamics. Technical Publication 88-7, water resource division, resource planning department, South Florida water Management District, West Palm Beach, p. 39

Skogen MD, Ji R, Akimova A, Daewel U, Hansen C, Hjøllo SS, et al. (2021) Disclosing the truth: are models better than observations? Marine Ecology Progress Series, in press. https://doi.org/10.3354/meps13574

Smyth D, Kregting L, Elsäßer B, Kennedy R, Roberts D (2016) Using particle dispersal models to assist in the conservation and recovery of the over-exploited native oyster (*Ostrea edulis*) in an enclosed sea lough. Journal of Sea Research 108:50–59

Suara K, Chanson H, Borgas M, Brown RJ (2017) Relative dispersion of clustered drifters in a small micro-tidal estuary. Estuarine, Coastal and Shelf Science 194:1–15

Sun D, Wan Y, Qiu C (2016) Three dimensional model evaluation of physical alterations of the Caloosahatchee River and estuary: impact on salt transport. Estuarine, Coastal and Shelf Science 173:16–25

Tay Y, Todd P, Rosshaug P, Chou L (2012) Simulating the transport of broadcast coral larvae among the Southern Islands of Singapore. Aquatic Biology 15:283–297

Volety AK, Savarese M, Tolley SG, Arnold WS, Sime P, Goodman P, Doering PH (2009) Eastern oysters (*Crassostrea virginica*) as an indicator for restoration of Everglades ecosystems. Ecological Indicators 9:S120–S136

Volety AK, McFarland K, Darrow E, Rumbold D, Tolley SG, Loh AN (2015) Oyster monitoring network for the Caloosahatchee Estuary. Final Report, South Florida Water Management District, West Palm Beach, Florida

Wallace RK, Waters P, Rikard FS (2008) Oyster Hatchery Techniques. Southern Regional Aquaculture Center, 4302. http://quilbay.com/wp-content/uploads/2014/08/CH-5-Hatchery-Techniques.pdf

Supporting Information

The following information may be found in the online version of this article:

Data S1. Supplementary methodological details.
Table S1. Continuous environmental data series available within the Charlotte Harbor estuarine system: data source, stations names, and parameters measured (RECON hourly, CHAP 15 minute) at the different stations.